

Measurement of sound field of ultrasound massager for the head in skull model

Shukan Okano¹, Yoshio Shimotori²
¹Institute of Biomaterials and Bioengineering, Tokyo Medical and Dental University,
²Research and Development Center, Kamiyama Mfg. Co., Ltd.

1. Introduction

Although ultrasound techniques are not novel, they are required to be highly safe and obliged to be examined by the medical device certification authority. Ultrasound massagers for the head were regarded as a novel medical device in strategy consultation with the Pharmaceuticals and Medical Devices Agency (PMDA)¹⁾ and measurements of sound wave propagation and sound distribution in a skull model became necessary as a basic study. Conditions of ultrasound therapeutic devices are specified by the Japanese Industrial Standards (JIS) T0601-2-5²⁾, in which a water tank model specified by the International Electrotechnical Commission (IEC) 61689 must be used for measurements³⁾. To our knowledge, no water tank for long-wave ultrasound measurement is available in Japan or any other country. Thus, we have prepared a water tank for measurement based on the IEC model and performed acoustic measurement of 30 kHz ultrasound vibrators. In addition, the sound distribution in skull models were measured.

Key words : ultrasound head massager, measurement of sound field, skull model

2. Objective

Regarding the influence of an ultrasound massager for the head on a human body, studies using brain waves, stress hormone, xenon computed tomography (CT)⁴⁾, heart rate, skin temperature, and circulatory dynamics⁵⁾ have been reported and a double blind randomized control trial (RCT) on autonomic nerve action⁶⁾ have been presented. However, no sound field measurement using an ultrasound vibrator of an ultrasound massager for the head or a skull model (3B Scientific Inc.) has ever been performed. The vibrator used in this study has a piezoelectric ceramic bimorph disc structure, in which vibration energy originating from the center while maintaining its intensity out to the periphery. The vibrating surface is made of acrylonitrile butadiene styrene (ABS) resin with a diameter of 28 mm, and inserted into a hair band and that is closely attached to the head.



Fig. 1 Ultrasound vibrator
 30 kHz frequency, vibrating surface with a 28-mm diameter, and 2 holding buttons

In this study, the frequency band has been predecided. A vibrator (Fig. 1) and an ultrasound massager for the head equipped with this were developed and the characteristics of this vibrator were measured. Then, to investigate the influence on the intracranial structures, a plaster-made phantom skull was fixed in a small-sized water tank (Fig.2) and one vibrator each were attached to the inner walls of the forehead and occipital region of the phantom skull. Vibration was then applied and the distribution of ultrasound propagation intensity was investigated.

In addition, another resin-made phantom skull model (Fig. 3) was fixed in a middle-sized water tank (Fig. 4), with one vibrator each attached to the outer walls of the forehead and occipital region. The propagation intensity distribution in the skull model was measured and the safety of the vibrator was investigated.



Fig. 2 Small-size water tank
 Water tank for the measurement of sound distribution in plaster-made phantom skull
 Phantom Size: 210 x 160 x 60 cm (W x D x H),
 Thickness: 2 cm

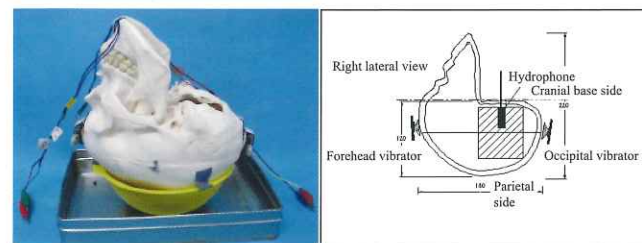


Fig. 3 Specially prepared resin skull model and size (mm)

3. Methods

1) Acoustic frequency of vibrator and measurement of characteristics

Since sound absorption by the medium is proportional to the square of the frequency⁷⁾, sound reaches deeper and to more distant sites as the frequency decreases. Although JIS, regarding ultrasound therapeutic devices, specifies that the lower limit of the ultrasound acoustic frequency to be 16 kHz and since the device is applied to the head to reduce auditory stimulation, we selected 30 kHz for

the acoustic frequency (f). This is about two times higher than the standard lower limit.

The following measurement method was employed to estimate the sound intensity radiated from the vibrator. Since the vibrator operation has sending-receiving reversibility, referring to the equivalent circuit⁸⁾ shown in Fig. 5-1, the vibrating parts (acoustic radiation surface) of the two vibrators (transmitting and receiving) were set facing each other and fixed with double-sided tape. An electrical input was added to the electric terminal of the first transmitting vibrator. Vibration produced in the vibrating part was received by the second receiving vibrator through electro acoustic conversion and the electrical output was taken from the second vibrator through acoustic-electric conversion. In actual vibrator output measurement, as shown in Fig.5-2, the transmitting and receiving vibrators were fixed in the air and the vibrator output was estimated

by measurement and calculation. Drive signals of the transmitting vibrator, V_i and I_i , and receiving vibrator input, V_o , in this measurement are shown as modulated waves and its magnified waveforms for reference in Figs. 6 and 7, respectively.



Fig. 4 Middle-size water tank
 Water tank for measurement of ultrasound intensity and sound distribution in skull model.
 Size: 70 x 40 x 35 cm (W x D x H)

Measurement of sound field of ultrasound massager for the head in skull model

The sound propagation velocity in the human body is equivalent to that in water and it is roughly 1,500 m / s⁹⁾.

Designating wavelength as λ , sound velocity as C , and frequency as f ,
 $\lambda = C / f$

Applying this to the conditions,
 $\lambda = 1,500 / 30,000 = 0.05 \text{ (m)} = 5 \text{ (cm)}$

Referring to the size, arrangement, and soundproof structure of the water tank model specified by

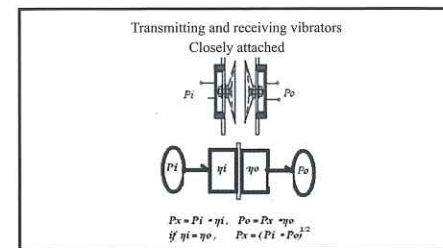


Fig. 5-1 Equivalent circuit of vibrator output measurement

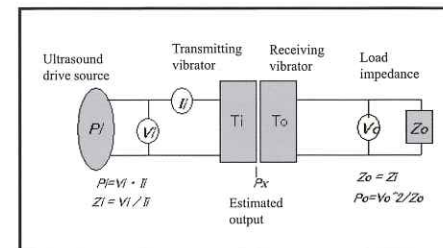


Fig. 5-2 Circuit structure used in vibrator output measurement

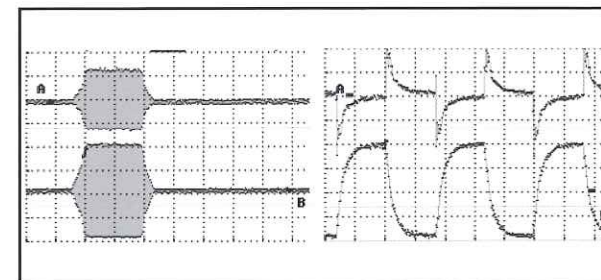


Fig. 6 Transmission-side vibrator-drive signal (100 ms / div.) and magnified waveform (10 μs / div.) (A: Current, B: Voltage)

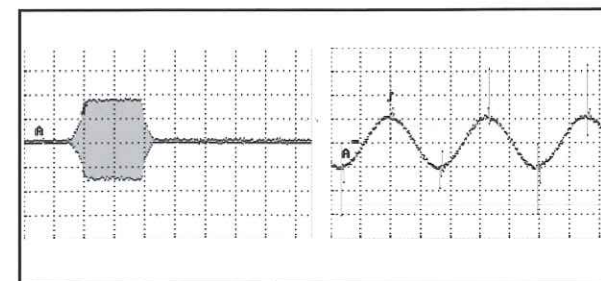


Fig. 7 Receiving-side vibrator waveform (100 ms / div.) and magnified waveform (10 μs / div.)

IEC61689, polyurethane waveform cushion was applied to the inner wall of the water tank of the middle-sized water acoustic measurement device (Fig.4) to prepare an experimental water tank suppressing reflection. Using this water tank, the intensity and characteristics of propagation attenuation of sound emitted by the vibrator received by a hydrophone were measured¹⁰⁾. The sound intensity and attenuation characteristics were measured in cooperation with Tokyo Metropolitan Industrial Technology Research Institute¹¹⁾.

In underwater acoustics, the sound intensity corresponding to 1 μPa sound pressure is set as the reference value (0 dB), but in the medical device field, it is presented as sound power passing through 1 cm² plane. Thus, 0.667 x 10⁻²² W / cm² was set as the reference value¹²⁾. The standard water density and underwater sound velocity is 1,000 kg / m³ and 1,500 m / s, respectively.

2) Measurement of sound distribution in plaster-made phantom skull using small-scale underwater acoustic measurement device

The vibrators were attached to the inner walls of the forehead and occipital region of the plaster-made phantom skull (prepared by the Department of Radiology, Fujita Health University) for calibration of X-ray CT of the head and fixed in the small-scale underwater measurement device (Fig.2).

Modulated waves of drive signals (Fig.6) were applied to the vibrator and the radiated ultrasound in the phantom was presented as a hydrophone signal was placed in front of the vibrator (Fig.9a).

Two vibrators attached to the inner walls of the forehead and occipital region of the phantom were simultaneously driven and the sound intensity synthesized underwater in the phantom was measured. The phase of the drive signal applied to the occipital vibrator was changed to 0°, 45°, 90°, 135°, and 180°(reverse phase against that on the forehead vibrator), and the distribution of the sound intensity synthesized under water in the phantom was measured to determine drive conditions in different phases.

3) Measurement of sound distribution in skull model using middle-sized underwater acoustic measurement device

The vibrators were attached to the forehead and occipital region on the external side of the skull model and fixed in the center of the middle-sized underwater acoustic measurement device (Fig.4).

The vibrators were driven at various phases as described in 3-2), and the distribution of the synthesized sound intensity in the skull model was measured.

The skull model was fixed under water with the parietal region at the bottom and the skull base at the top. To insert the hydrophone and perform scanning measurements, the foramen magnum was extended and cut into a rectangle (width : 25 mm, length : 60 mm). The anteroposterior and vertical distributions of synthesized sound intensity were measured centering the foramen magnum.

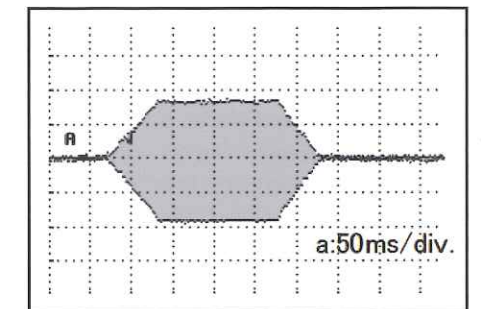


Fig. 9-a Hydrophone signal Modulated wave

4. Results

1) Measurement of characteristics of ultrasound vibrator

Fig.5-2 is the 'circuit structure used for vibrator output measurement' which is used for convenience for specific measurement based on the equivalent circuit (Fig.5-1). The permissible maximum output of the ultrasound massager for the head was adopted as the ultrasound drive source, in which T_i represents the transmitting vibrator and T_o represents the receiving vibrator. P_i represents the ultrasound drive output, I_i represents the root mean square (rms) value on a drive current ammeter, V_i represents rms on a drive voltmeter, and V_o represents the rms value of the input voltage received by the receiving vibrator and added to load impedance, and Z_o , on an input voltmeter. Since the vibrators are made of ceramics with a volume load, the rms value of P_i cannot simply be determined because of various phases between the voltage and current. However measurement was performed to obtain a rough indication.

Measurement of sound field of ultrasound massager for the head in skull model

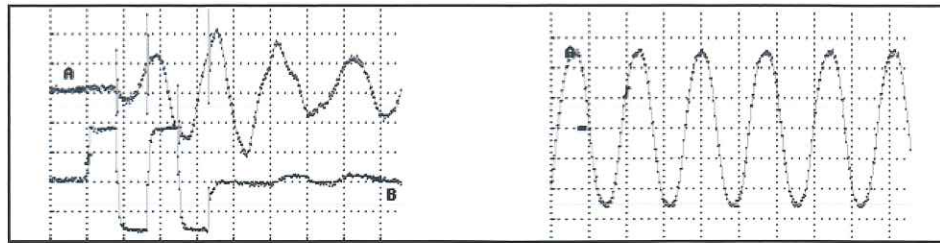


Fig. 8 Wave received by the hydrophone in sound intensity measurement
The left figure shows two waves (pulse wave $20 \mu s / div.$) and the right figure shows the modulated wave (continuous wave $20 \mu s / div.$). In the left figure, signal B comprised of two waves driving the vibrator and relative position and relative waveform of hydrophone signal A at a 10 mm distance are presented.

The measurement and calculated results are as follows:

Transmitting (primary) side : Receiving (secondary) side
 $V = 15.8 \text{ V rms } I = 0.304 \text{ A rms } : V_o = 0.165 \text{ V rms } Z_o = 52 \Omega$
 $Z_i = V_i / I_i = 52 \Omega P_i = V_i * I_i = 5.7 \text{ W} : P_o = V_o^2 / Z_o = 0.52 \text{ mW}$

The drive signal applied to the transmitting vibrator is shown in Fig. 6 and the waveform of the receiving vibrator is shown in Fig. 7.

The output of the transmitting vibrator, P , was determined as follows.

The electroacoustic conversion efficiency (η_i) of the vibrator and electroacoustic conversion efficiency (η_o) were regarded as $\eta_i = \eta_o$.

$P_x = P_i * \eta_i$ becomes from $\eta_i = P_x / P_i$,
 $P_o = P_x * \eta_o$ is substituted to $P_o = P_x * P_x / P_i$, and
 $P_x^2 = P_o * P_i$ is led to $P_x = (P_o * P_i)^{1/2}$ —Equation 1

Substituting the measured values in Equation 1, the transmitting vibrator output was determined as follows:

$P_x = \sqrt{5.7 \text{ W} * 0.52 \text{ mW}} = 54 \text{ mW}$.

The disk-shaped vibrator surface with a 28 mm diameter and its area, S , was calculated as 6.15 cm^2 by applying πr^2 . The intensity of sound generated in the medium (water) on the transmitting vibrator surface was estimated as $8.78 \text{ mW} / \text{cm}^2$ by applying P_x / S .

The characteristics of the vibrator in water were measured at the Tokyo Metropolitan Industrial Technology Research Institute. The middle-sized underwater acoustic measurement device was taken to the institute and the intensity of sound generated in water, its distribution, and propagation attenuation characteristics were measured⁽¹¹⁾. Since sound intensity must be measured before

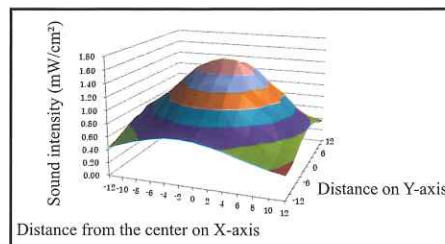


Fig. 10 Sound distribution on the vibrator surface
Vibrator surface diameter: 28 mm, 30 kHz, 4.4 mW drive

wave reflection from the wall, as shown in Fig. 8, pulse wave B comprised of two waves were applied. Considering reflection from the wall, the minimum reciprocating distance was 30 cm. Accordingly, when the wavelength is 5 cm, the test had to be performed within a six-wave pulse, and this test was performed with a two-wave pulse. The wave received by the hydrophone placed at a 10-mm distance is shown as A on the left in Fig. 8 for reference. For the sound intensity, $1/\sqrt{2}$ of the larger wave of the two waves was adopted as the root mean squared value. In addition, the signal of the continuous wave received by the hydrophone at a 5 cm site in response to applying the modulated wave is shown on the right in Fig. 8.

The intensity distribution of sound generated in water by the vibrator was cone-shaped, as shown in Fig. 10, and the maximum intensity at the center of the vibrator was $1.6 \text{ mW} / \text{cm}^2$. The vibrator was a round-shaped disk with a 28 mm diameter with a mean output from the radiation surface of $0.71 \text{ mW} / \text{cm}^2$. The effective radiation output was calculated using the equation below:

Effective radiation output = Mean output from the radiation surface * radiation area
 $= 0.71 \text{ mW} / \text{cm}^2 * \pi(1.4 \text{ cm})^2$
 $\approx 4.4 \text{ mW}$

The characteristic of underwater sound transmission attenuation roughly indicating penetrance is shown in Fig. 11. The distance at which the maximum sound pressure level attenuated to $1/10$ was about 5 cm (corresponding

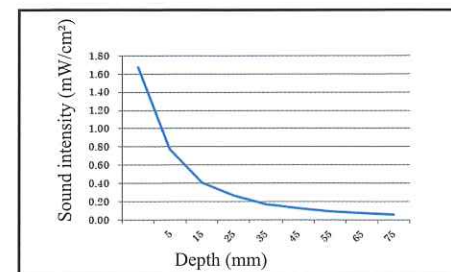


Fig. 11 Measurement of attenuation of underwater ultrasound propagation
30 kHz, 4.4 mW drive

to one wavelength).

The horizontal (x-axis) distribution of 3-dimensional underwater sound propagation was investigated at a 5 cm anterior site (corresponding to one wavelength). The results are shown in Fig. 12-1. For simultaneous comparison of Fig. 10 and Fig. 12-1, these are presented with a uniformed scale in Fig. 12-2. The intensity of sound radiated from the vibrator was strongest at a distance of 5 mm with limited sound distribution, and decreased at a distance of 50 mm with a wider distribution.

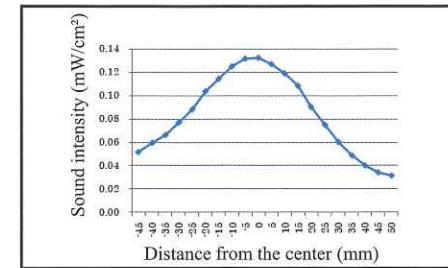


Fig. 12-1 Horizontal distribution at 50 mm front from the vibrator surface

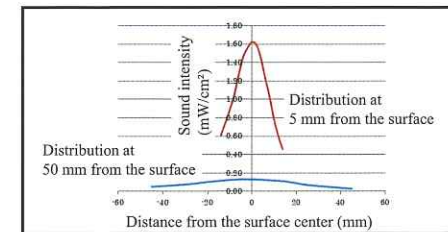


Fig. 12-2 Diffusion distribution from the vibrator as a sound source
Horizontal distribution at 5 and 50 mm front from the vibrator surface
30 kHz, 4.4 mW drive

2) Measurement of sound distribution in plaster-made phantom skull

The maximum output was simultaneously applied to both vibrators while attached to the inner surface of the forehead and occipital region facing each other in the anteroposterior direction in the plaster-made phantom skull, the phase was set to the same and reverse phases, 45° , 90° , and 135° , and the

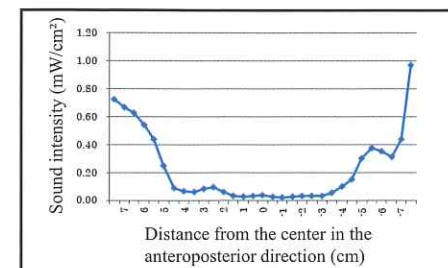


Fig. 13 Acoustic distribution in plaster-made skull phantom
Forehead + occipital vibrators driven
Mean acoustic distribution of the sum of the same and reverse phases
30 kHz, 4.4 mW drive

Measurement of sound field of ultrasound massager for the head in skull model

intensity distributions of synthesized sounds were investigated. No change due to the phase difference was noted in the intensity of the phantom's center, but the distribution had varied along the wall. The mean distribution of the sum of the same and reverse phases is shown in Fig. 13. Compared with the same or reverse phase alone, the distribution was balanced. The intensity was high on both walls of the forehead and occipital region, whereas it was flat and low pan-shaped in the central region.

The distribution toward the bilateral temporal regions (lateral direction) in the plaster-made phantom skull was also investigated. Similar to that in the anteroposterior direction described above, the sound intensity distribution also rose near the walls.

3) Measurement of sound distribution in skull model

The maximum output was simultaneously applied to the vibrators attached to the outer surfaces of the forehead and occipital region in the skull model shown in Fig.3. The phase was set at the same and reverse phases, 45° , 90° , and 135° and the distributions of synthesized sounds in the anteroposterior direction were measured centering the foramen magnum. The sound distribution from the forehead toward the foramen magnum was generally low regardless of the phase difference, but variation due to the phase difference appeared as the position came closer to the occipital region. The mean distribution of the sum of the same and reverse phases is shown in Fig.14. The sound intensity was $3 \mu W / \text{cm}^2$ in the forehead, reached a peak of ($22 \mu W / \text{cm}^2$) in the region posterior to the foramen magnum, and it was $8 \mu W / \text{cm}^2$ in the occipital region. The distribution was chevron-shaped near the central region with an intensity that was five times higher compared with the flatter shape of its periphery. Then, the distribution in the parietal region and cranial base (vertical direction) was measured from the foramen magnum. The distribution was chevron-shaped in both the central region and the vertical direction with a sound intensity in the intracranial space of $10 \mu W / \text{cm}^2$.

5. Discussion

The ultrasound output of the vibrator was different between that from closely contacted transmitting and receiving vibrators in the air and that in the water tank measured by the hydrophone. The values were 54 and 4.4 mW, respectively, showing a 12.3 times lower difference. Measurement in the water tank, at a 5 mm distance from the vibrator surface, corresponding to $1/10$ of the wavelength, its sound intensity in the central region reaching its maximum was $1.6 \text{ mW} / \text{cm}^2$ and this value was $1 / 1,875$ of the maximum output intensity, $3 \text{ W} / \text{cm}^2$, specified by JIS for ultrasound therapeutic devices. The intensity of sound leakage is limited to $100 \text{ mW} / \text{cm}^2$ or lower by JIS. Thus, the sound intensity employed in this study was a very low level.

Regarding the experimental water tank used for measurement, firstly, the acoustic reflection was large in the plaster-made phantom skull and standing waves of acoustic echo were noted as shown in Fig. 9-c, whereas waves were anechoic in the middle-sized underwater acoustic measurement device as shown in Fig. 9-b, clarifying that the waveform cushion used in the middle-sized underwater acoustic measurement device was effective, being an appropriate measurement environment of acoustic output with a relatively low intensity.

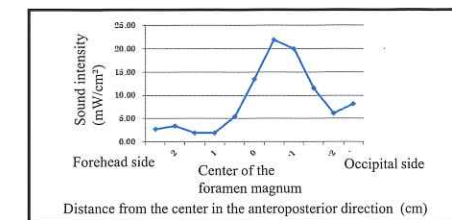


Fig. 14 Acoustic distribution in skull model
Forehead + occipital vibrators driven
Mean acoustic distribution of the sum of the same and reverse phases
30 kHz, 4.4 mW drive

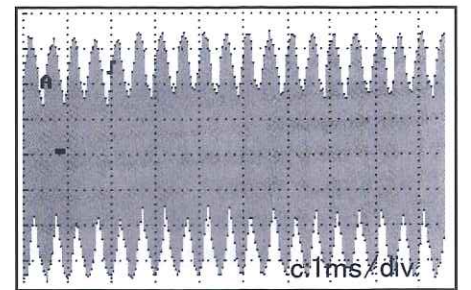


Fig. 9-c Hydrophone signal
Echoic standing waves in plaster-made skull phantom

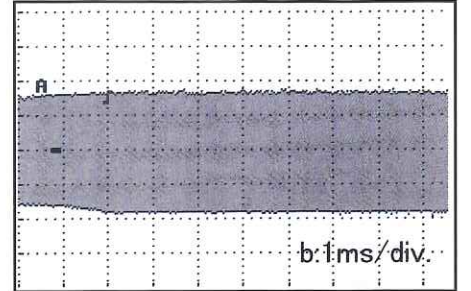


Fig. 9-b Hydrophone signal
Anechoic waves

Low-frequency ultrasound is considered to have strong penetration ability and is to be avoided, but the position at which the sound intensity of 30 kHz decreased to $1/10$ was about 5 cm and this corresponded to one wavelength, clarifying that it does not have strong penetration ability exceeding the skull size.

When reflection of ultrasound from the inner wall and the distribution of standing waves in the plaster-made phantom skull were investigated, the sound intensity increased near the forehead and occipital region compared with that in the central region of the brain, showing a pan-shaped distribution. The intensity near the bilateral temporal walls of the plaster-made phantom skull also showed a pan-shaped distribution similar to that in the forehead and occipital region. The increases near the walls may have been due to reflected waves.

The sound intensity distribution in the skull model was investigated. A chevron-shaped distribution showing an increase in the sound intensity in the intracranial central region slightly deviated from the foramen magnum toward the occipital region. The intensity in the anteroposterior direction was $22 \mu W / \text{cm}^2$ and that in the vertical direction at the foramen magnum was $10 \mu W / \text{cm}^2$, being very low.

Measurement of sound field of ultrasound massager for the head in skull model

6. Conclusion

The intensity of sound generated in water by the 30 kHz ultrasound vibrators used in this study was $1 / 1,875$ of the maximum output specified by JIS for ultrasound therapeutic devices for heat treatment, and the sound intensity in the skull model was very low ($22 \mu W / cm^2$ or lower), which is a safe level. Regarding the characteristics of the vibrator, it is light, not stressful when it is closely attached to the head, and simple to use without the use of any gel. The details are described in the granted patent¹³⁾.

It is desirable for all medical devices that a maximum effect can be obtained at a low output to achieve the objective. Clarification of an increase in cerebral blood flow by non-thermal action of ultrasound treatment may promote development of low-frequency ultrasound therapeutic devices.

As a task to be solved in the future, it is necessary to investigate the influence of very weak ultrasound vibration on human brain diseases based on the findings of the experiments using the plaster-made phantom skull and skull model.

Acknowledgment

We are grateful to Mr. Tsuneo Kikuchi, Head of Laboratory, and Mr. Masahiro Yoshioka, Acoustics and Ultrasound Standards Group, Research Institute for Measurement and Analytical Instrumentation, National Institute of Advanced Industrial Science and Technology, for providing us with documents of IEC 61689-based sound field measurement and allowing us to observe water tanks, Mr. Koichi Kanda, Chief, and Mr. Toru Miyairi, Photoacoustic Technology Group, Tokyo Metropolitan Industrial Technology Research Institute, for their engagement in vibrator characteristics measurement in the water tank, and engineers of TOYO Corporation for cooperation in preparation of the hydrophone and water tank.

References

- 1) Announcement from the director of Pharmaceuticals and Medical Devices Evaluation Center # 0701006. Independent Administrative Agency. Pharmaceuticals and Medical Devices Agency (PMDA). 2013.
- 2) Individual requirements regarding the safety of ultrasound physical therapeutic device. JIS T0601-2-5 : 2005 / IEC 61102.
- 3) Yoshioka M. Measurement of sound field based on IEC 61689. Advanced Industrial Science and Technology. Amended Pharmaceutical Affairs Act. 2005.
- 4) Shimotori Y, Watayo T, Okano S. Health promoting effect by head ultrasound massager. Health Sciences. 2007. 23(4). p 274.
- 5) Okano S, Shimotori Y, Watayo T. Effects of ultrasound vibration on human EEG and blood circulation. J. Physiol. Sci. 2008, Vol. 58 (Suppl.), p. S98.
- 6) Uebaba K, Xu F, Yatsuka S, Kim J. Double blind RCT test of ultrasound head massage on autonomic nerve function. Thirty third annual meeting of Japan Ayurveda Society. 2011.
- 7) Propagation / absorption of sound wave within a body. Revised edition of Handbook of Medical Ultrasound Device. Incorporated association of Japan Electronic Machine Industry Association. Corona Co Ltd. p 19. 1997.
- 8) Signal transmission equivalent circuit to obtain gain of sending-receiving wave, sending-receiving wave system by two transducer and sending-receiving wave of transducer. Revised edition of Handbook of Medical Ultrasound Device. Incorporated association of Japan Electronic Machine Industry Association. Corona Co Ltd. p 27. 1997.
- 9) Acoustic characteristics for ultrasound of the body parts / sound velocity in blood and adipose. Revised edition of Handbook of Medical Ultrasound Device. Incorporated association of Japan Electronic Machine Industry Association. Corona Co Ltd. p 35. 1997.
- 10) Standard Transducers & Hydrophones. Catalog of RESON Co Ltd. Hydrophone TC4013. Sensitivity: 30 kHz / -211.8 db. Preamplifier. EC6081
- 11) Features of vibrator on ultrasound head massager. Tokyo Metropolitan Industrial Technology Research Institute. #25. 70(8). 2013.
- 12) Unit Conversion. Catalog of RESON Co Ltd. p 105-106.
- 13) Disease prevention system for cerebral nervous system. Japanese Patent # 4162097. 2008